

Electrolyte Induced Electrical Dis-connection between Single Graphene Nanoplatelets and an Electrode

Atiweena Krittayavathananon^{a,b,†}, Xiuting Li^{a,†}, Christopher Batchelor-McAuley^a, Montree Sawangphruk^b, Richard G. Compton^{a}*

^aDepartment of Chemistry, Physical and Theoretical Chemistry Laboratory, University of Oxford, South Parks Road, Oxford OX1 3QZ, UK.

^bDepartment of Chemical and Biomolecular Engineering, School of Energy Science and Technology, Vidyasirimedhi Institute of Science and Technology, Rayong 21210, Thailand

Corresponding Author

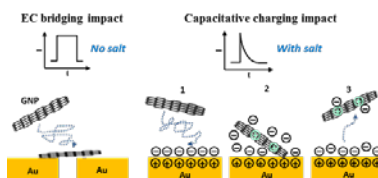
*Correspondence to: richard.compton@chem.ox.ac.uk

Telephone number: +44)0(1865 275957

ABSTRACT

We report the influence of electrolyte on the electrical contact between graphene nanoplatelets (GNPs) and an electrode via a single entity electrochemical technique. The current ‘steps’ were observed in the absence of electrolyte due to the GNPs impacting on and bridging across an interdigitated gold electrode array (IDE), in contrast current spikes of short duration were obtained in the presence of electrolyte. This result indicates that in the latter case the constant short circuit bridging current was switched off and replaced solely by impacts of GNPs with single electrodes. These observed current spikes measured in the presence of electrolyte are evidenced to be of a capacitative nature, demonstrating the high sensitivity of the electronic properties of the GNPs/metal junction to the ionic strength of the electrolytic solution.

TOC GRAPHICS



Graphene as one of the most important carbon nanomaterials has attracted significant attention due to its enhanced electrical and thermal conductivity, large surface area, higher charge mobility and carrier concentration, and mechanical strength.¹⁻² Graphene nanoplatelets (GNPs) enjoy the advantageous properties of single-layer graphene but avoid the poor stability because of their high ordered graphitic structures.³ This allows their widespread applications in sensing and energy storage technologies.⁴⁻⁵ One of these important applications is to work as catalyst and catalyst support for various electrochemical reactions.⁶⁻¹⁰ To achieve high performance for catalysis, intensive efforts have been made to improve the chemical and physical properties of the GNPs.⁶⁻¹⁰ However, the aim cannot be readily achieved without addressing the fundamental problem of forming a high-quality contact with the electrode substrate.¹¹⁻¹² It is therefore essential to properly quantify the GNPs-electrode contact and further to understand how the GNPs-electrode contact is affected by their surrounding environment, such as commonly used electrolytic solutions, to assist their applications. When studying interfacial redox reactions, the use of supporting electrolyte is near ubiquitous. The electrolyte serves to contract the electrochemical double layer to length scales comparable to the electron tunneling distance and ensure that a significant potential gradient does not build-up in the depletion zone surrounding the electrode.¹³⁻¹⁴ However, the presence of electrolyte can lead to the properties of the GNPs-electrode interface to be altered due to the charged functional groups on the GNPs surface and therefore affect their performance in applications.¹⁵⁻¹⁶

Conventional electrochemical techniques involve multilayer or monolayer formations of the catalyst on the electrode surface and usually ignore the contact resistance between them, which increases the complexity of analysing electrical connectivity.¹⁷⁻¹⁸ Direct information regarding the connectivity of an individual nanomaterial to an electrode surface is not readily obtainable via the conventional methods which usually require complicated device fabrication and can only enable the *ex-situ* measurement of a single or a few nanomaterials in an experiment.¹⁹⁻²⁰ To better understand the contact properties of carbon nanomaterial/metal interface, our previous work has developed a simple, statistical and non-destructive technique based on the ‘nano-impact’ methodology to quantify the connectivity of an individual carbon nanomaterial to a metal electrode.²¹⁻²⁴ In these experiments an interdigitated electrode array with a gap of a few microns is immersed in a suspension of carbon nanoparticles, such as nanotubes or GNPs. Upon diffusion and impact to the array, the particles may form a bridge across two adjacent microbands so that a constant short circuit current will arise when a potential is applied across the two band arrays. The work presented herein seeks to use this single entity technique to understand how the presence of variable levels of an electrolyte (NaCl) in low concentrations can influence the behaviour of the GNP/Au contact. This is an early stage research work focusing on one of the main influencing factors to the GNP/electrode contact. NaCl as representative electrolyte was investigated and a binder-free system was applied. More comprehensive study on the material/electrode contact including the effect of the nature of the electrolyte and the influence of the commonly used binders in the practical applications can be conducted in future.

The electrochemical bridging-impact of GNPs was first conducted in the absence and presence of electrolyte (NaCl). In order to break the GNPs aggregates, a $2.64 \times 10^{-15} \text{ mol dm}^{-3}$ GNPs suspension was sonicated in an ultrasonic bath (230V 50/60Hz 150W) for 20 min. The

average size of the GNPs was obtained from the optical microscope images and is found to be in the range of 7~9 μm (Figure S1), which is large enough to bridge two neighboring bands of the IDE-Au. Both the band and gap are 5 μm . The IDE-Au was immersed into the GNPs suspension which has been exposed to variable concentrations of NaCl (0-200 μM) for different times (0-120 min). Chronoamperometry was performed at a constant potential of 0.8V in a two-electrode system with one of the two band arrays of the IDE-Au acting as the working electrode and the other as the reference and counter electrodes. The representative chronoamperometric profiles of the GNPs suspensions aged for 2 hour with different concentrations of NaCl are shown in Figure 1A. In the right-hand side zoom-in profiles, the current impacts appear as ‘steps’ or ‘spikes’ above the background and were observed in all cases. No such current transient features were observed in the absence of GNPs (Figure S2), indicating that the current transients shown in Figure 1A arise from the impacting of GNPs on the electrode. In the absence of NaCl, characteristic ‘steps’ are observed in the chronoamperograms, which is consistent with the results of our previous reports²¹⁻²² and can be ascribed to the arrival of the GNPs bridging the neighbouring bands of the IDE-Au, leading to the short circuit current passing through the GNPs with the potential applied across the two band arrays of the IDE-Au. With an increase of the concentration of NaCl, the shape of the current impact changes from a ‘step’ to a ‘spike’. Specifically, the duration of the impacts decreases from ~150 ms to ~20 ms when the electrolyte (NaCl) concentration increases from 0 to 200 μM (Figure S3a). Moreover, the magnitude of the current impacts significantly drops by an order of magnitude in the presence of NaCl for concentrations ranging from 75 to 200 μM . For higher concentrations of NaCl, even smaller current spikes are observed. The phenomenon is also observed in the GNPs suspensions aged for different time, as shown in Figure 1B. The increasing trend of the current magnitude with aging

time is ascribed to the aggregation/agglomeration of the GNPs, which has been demonstrated in our previous work.²² As shown in Figure S3a, the duration of the GNP impact in the absence of NaCl increases from around 60 ms to 130 ms as the aging time increases from 0 min to 120 min; this may result from the longer bridge landing and/or better contact of the formed GNPs aggregate on the electrode surface. In the presence of electrolyte, the impact duration remains constant as the aging time increases, indicating the different nature of the GNPs impact with the electrode from that in the absence of electrolyte.

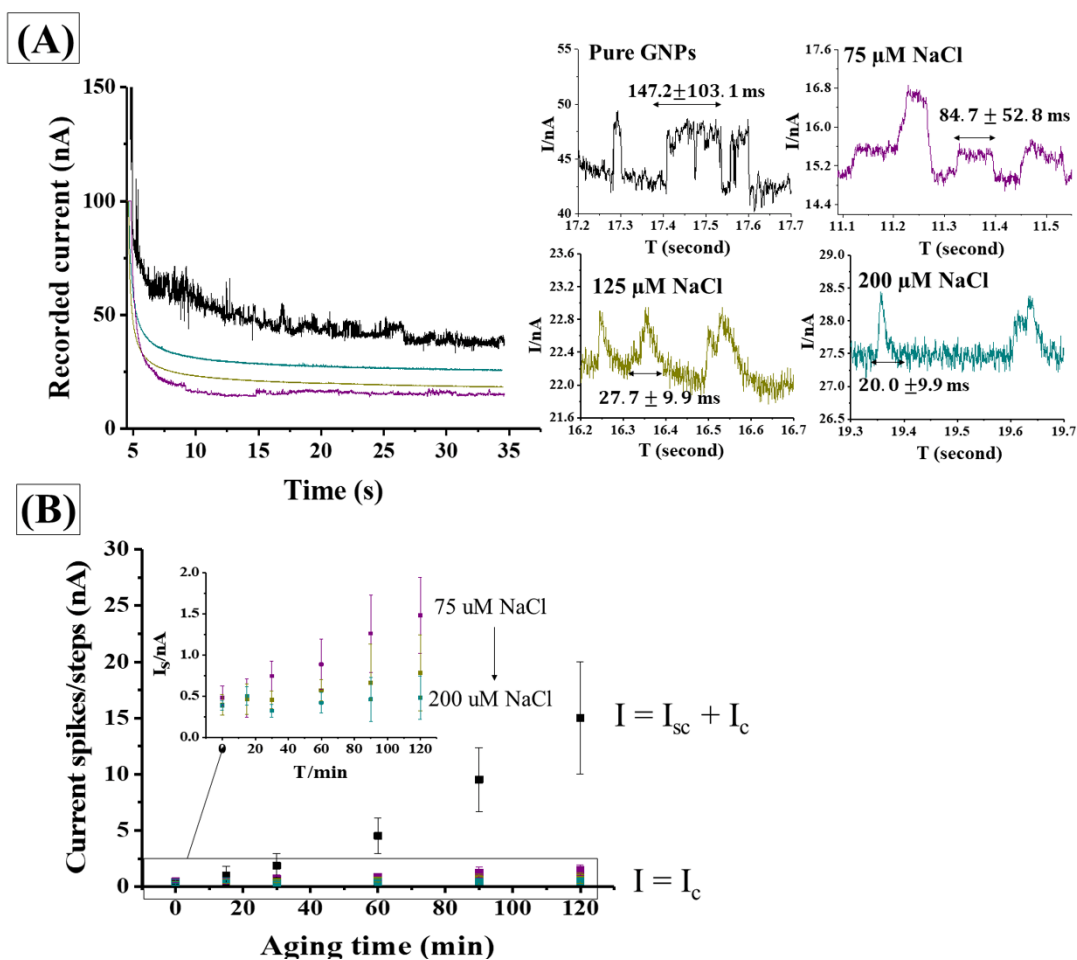


Figure 1. (A) Chronoamperometric profiles of IDE-Au immersed in a 2.64×10^{-15} mol.dm³ GNPs suspension containing different concentration of NaCl (0-200 μM) at a constantly applied potential of 0.8V after aging GNPs in the solution for 2 hour and (B) Average current of steps/spikes against aging

time of GNPs suspension with 0.8V applied to the two band arrays of the IDE-Au. I_{sc} and I_c represent the short circuit current and capacitive current respectively.

Having evidenced that the current impacts obtained in both absence and presence of electrolyte were related to the GNPs in solution and the clear difference of the impacts in these two cases, the physical origin of these charge transfer processes was further investigated. As discussed in the previous section, in the presence of NaCl, the current transients is ‘spike’ shaped instead of ‘step’ shaped and the magnitude significantly differs. This likely means that the effective bridging electrical contact between the GNPs and electrode is switched off by the electrolyte, and therefore there is no constant short circuit current (‘step’) passing through the landing GNPs. Since the lack of redox activity of the used GNP has been evidenced previously,²⁵ the GNPs do not significantly contribute to the impact charge faradaically. Thus, the observed short transient current features likely result from the ‘capacitive’ charging impact due to the collision of the GNPs with the electrical interface.

In order to clarify this, a capacitive impact experiment was next investigated with a three-electrode system. Two bands of IDE-Au were connected and used as a working electrode inserted into $2.64 \times 10^{-15} \text{ mol dm}^{-3}$ GNPs suspension which contains different concentrations of NaCl. Ag and Pt wires are used as reference and counter electrodes, respectively. A series of potentials between -0.7 and 0.7 V vs. Ag were applied to the working electrode, the corresponding chronoamperograms were recorded. Figure S4 shows the representative chronoamperometric profiles at -0.7, -0.5, +0.5 and +0.7V in the presence of 0 μ M and 200 μ M NaCl. Current spikes from the GNPs were observed in all the cases. Around 25-30 current spikes were collected at each potential. The logarithm (\log_{10}) of the absolute mean integrated charge passed during an impact event as a function of potential is shown in Figure 2. The black and

green squares in Figure 2 represent the charge of spikes collected in the presence of 0 μ M and 200 μ M NaCl respectively. In both cases, it is found that with the increasing magnitude of the applied potential, the spike charge of the capacitive impacts steadily increases. This is because the impacting particle removes more charge from the electrode–electrolyte interface as a higher magnitude of potentials is applied. It suggests the capacitive nature of the impact spikes observed. The charge magnitude of the GNP impacts over the potentials of study is in the range of 0.1-21.0 pC and 5.6-65 pC in 0 μ M and 200 μ M NaCl respectively. For comparison, variable potential study was also conducted in the ‘bridging’ experiment, where GNPs suspensions containing 0 μ M and 200 μ M NaCl was investigated respectively at an IDE-Au electrode with different potential applied across its two microband arrays. Figure S5 shows the average charge of the GNPs impacts against the applied potential. The values in the presence of 200 μ M NaCl is in the range of 5.6-18 pC, which is in the same order of magnitude as that (5.6-65 pC) obtained in the above capacitive impact experiment. This further confirms that ‘spike’ shaped impacts obtained in the presence of electrolyte in the bridging experiment are of capacitive origin. Moreover, the relation between the duration of the impacts from the bridging experiment and the applied potential difference in the absence of electrolyte was analyzed. As shown in Figure S6, the impact duration decreases with the increase of the applied potential, further indicating that the influence of the double layer on the electro-connectivity of the GNPs to the electrode surface. Note that for the bridging experiment using the two-electrode system, whether a GNP impacts at the anode or the cathode, the resulting capacitive current will be of the same polarity and so the experiment is insensitive to which electrode the event occurred at.

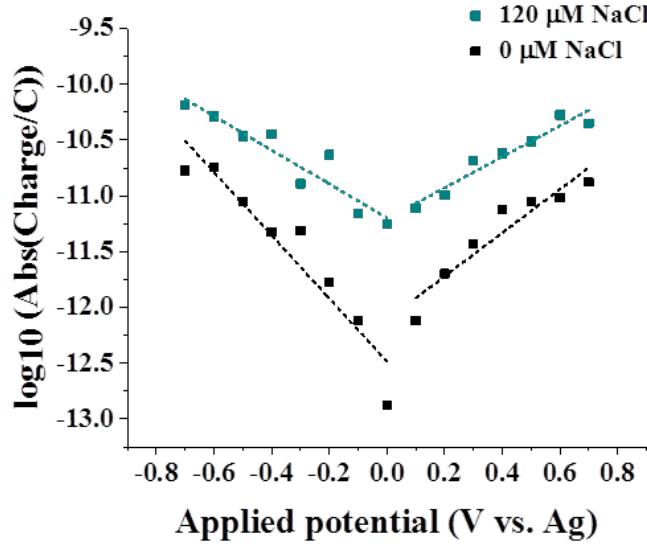


Figure 2. The absolute charge of GNPs impacts shown with a logarithmic (\log_{10}) scale plotted against applied potential (vs. Ag) in GNPs in pure water (-) and GNPs in 200 μM NaCl (-). Note that the sign of the charge recorded in the potentials left than the point of intersection is negative (reductive) and right than the point of intersection is positive (oxidative).

Capacitance is an important parameter to indicate the electronic properties of carbon materials. The differential capacitance can be calculated using the slope of the charge vs. applied potential following eq. (1).

$$C_d = \frac{1}{A} \left(\frac{\partial q}{\partial \varphi} \right)_{\mu, T, p} \quad (1)$$

where q is surface charge, φ is the electrode potential and A is the area ($6.8 \times 10^{-7} \text{ cm}^2$) of the GNPs derived from the average GNPs width (8.2 μm) in the optical microscope images. The differential capacitance value of the GNPs impact in 0 μM and 200 μM NaCl is in the range of tens of $\mu\text{F}/\text{cm}^2$ respectively, slightly higher than that⁴ for graphene and similar carbon materials reported in literature.²⁵⁻²⁷ This is likely due to the underestimation of the geometry size of the GNPs from the optical microscope images. Adding electrolyte into the system increases the ionic strength of the solution, decreasing Debye length and resulting in the increase of the capacitative

charge as expected by the Gouy-Chapman theory.²⁸⁻²⁹ The capacitance increase of GNPs in the presence of electrolyte may be also partially contributed to the electro-attraction between the negatively charged surface functionalities of the GNP³⁰ and the cations (Na^+) in the solution.³¹

The similarity between the capacitive impacts from the three electrode system and the short current transients (spikes) obtained in the presence of electrolyte from the two electrode system indicates that the latter is dominated by the capacitive charging. The short circuit current from the GNPs bridging electrical contact observed in the absence of electrolyte is switched off in the presence of electrolyte. The behaviour of the GNPs impact in these two cases is illustrated in Figure 3. In the absence of electrolyte, the obtained current impact (I) of GNPs comes from either a short circuit current (I_{sc}) where GNPs are landing across a gap of IDE-Au and/or capacitance charging current (I_c). The capacitance charging current (I_c) is low in comparison to the current magnitude of the bridging impact. Short circuit impacts show a ‘step’ behaviour and the step current increases with respect to the applied potential, $V=IR$. In the presence of the electrolyte, the corresponding high electric field in the vicinity of the interface results in a more ordered water layer, leading to the increased distance of closest approach repulsion between GNP and electrode and therefore the short circuit electrical contact is switched off. Hence, the capacitance charging plays a dominant effect on the GNPs impacts in the presence of the electrolyte.

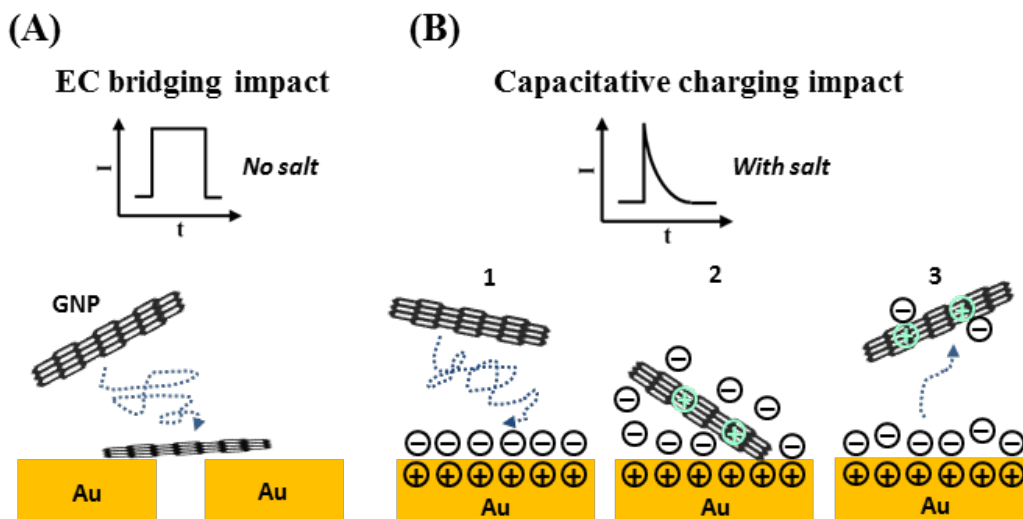


Figure 3. Schematic of (A) electrochemical bridging impact in the absence of electrolyte and (B) capacitive impact in the presence of electrolyte. Note that in the case of (B) other mechanisms are possible³² and is illustrated in Figure S7.

In conclusion, an electrolyte effect of the GNP/metal contact has been demonstrated using the ‘nano-impact’ method. In the presence of the electrolyte, the shape of the GNPs impacts changes from ‘step’ to ‘spike’ and the current magnitude significantly drops. **This is attributed to the increased distance of closest approach repulsion between GNP and electrode in the presence of electrolyte due to the formation of more ordered water layer at the interface in the high electric field.** The GNPs/metal short-circuit electrical contact is therefore switched off in the presence of the electrolyte, and the capacitive charging becomes dominant in the GNPs impacts. The electronic properties of the GNPs/metal junction are very sensitive to the ionic strength of the electrolytic solution.

ASSOCIATED CONTENT

AUTHOR INFORMATION

Corresponding Author

*E-mail: richard.compton@chem.ox.ac.uk. Telephone: +44(0) 1865 275957

Author Contributions

[†]A.K. and X.L.: These authors contributed equally to this work.

Notes

The authors declare no competing financial interests.

ACKNOWLEDGMENT

This project has received funding from the European Research Council (ERC) under the European Union's Horizon 2020 research and innovation programme (grant agreement No. 727292) and from the European Research Council under European Union's Seventh Framework Programme)FP/207-2013(, ERC Grant Agreement no. 320403. A.K. gratefully acknowledges funding from the Thailand Research Fund)RSA5880043(and Vidyasirimedhi Institute of Science and Technology.

Supporting Information

Supporting Information consists of experimental section and supporting figures. The supporting figures include bright-field optical microscopic images GNPs in solution with and without out electrolyte, chronoamperometric profiles of IDE-Au immersed in water and NaCl without the GNPs at 0.8V, average duration of current steps/spikes resulting from the bridging-impact of GNPs in different concentrations of NaCl vs. aging time, chonoamperometric profiles of

capacitive-impacts at different applied potentials using the three electrode system in GNPs suspension containing 0 μ M and 200 μ M NaCl at -0.7, -0.5, 0.5 and 0.7 V (vs Ag), average charge of the GNPs impacts against the applied potential across two bands of IDE-Au in the presence of 0 μ M and 200 μ M NaCl, average duration of current steps/spikes from the electrochemical bridging-impact of GNPs at the different applied potentials in the absence of electrolyte, and schemitic illustration of two possible processes involved in the experimental capacitive impacts. The Supporting Information is available free of charge on the ACS Publications website.

REFERENCES

- (1) Pumera, M. Electrochemistry of Graphene, Graphene Oxide and Other Graphenoids: Review. *Electrochem. Commun.* **2013**, 36, 14-18.
- (2) Ambrosi, A.; Chua, C. K.; Bonanni, A.; Pumera, M. Electrochemistry of Graphene and Related Materials. *Chem Rev* **2014**, 114, 7150-88.
- (3) Liu, L.; Ryu, S.; Tomasik, M. R.; Stolyarova, E.; Jung, N.; Hybertsen, M. S.; Steigerwald, M. L.; Brus, L. E.; Flynn, G. W. Graphene Oxidation: Thickness-dependent Etching and Strong Chemical Doping. *Nano Lett* **2008**, 8, 1965-70.
- (4) Han, J.; Zhang, L. L.; Lee, S.; Oh, J.; Lee, K. S.; Potts, J. R.; Ji, J.; Zhao, X.; Ruoff, R. S.; Park, S. Generation of B-doped Graphene Nanoplatelets Using a Solution Process and Their Supercapacitor Applications. *ACS Nano* **2013**, 7, 19-26.
- (5) Kavan, L.; Yum, J. H.; Gratzel, M. Graphene Nanoplatelets Outperforming Platinum as the Electrocatalyst in Co-bipyridine-mediated Dye-sensitized Solar Cells. *Nano Lett* **2011**, 11, 5501-6.
- (6) Bui, H. V.; Grillo, F.; Helmer, R.; Goulas, A.; van Ommen, J. R. Controlled Growth of Palladium Nanoparticles on Graphene Nanoplatelets via Scalable Atmospheric Pressure Atomic Layer Deposition (Retracted article. See vol. 122, pg. 9256, 2018). *J. Phys. Chem. C* **2016**, 120, 8832-8840.
- (7) Ju, M. J.; Jeon, I.-Y.; Kim, H. M.; Choi, J. I.; Jung, S.-M.; Seo, J.-M.; Choi, I. T.; Kang, S. H.; Kim, H. S.; Noh, M. J.; Lee, J.-J.; Jeong, H. Y.; Kim, H. K.; Kim, Y.-H.; Baek, J.-B. Edge-selenated Graphene Nanoplatelets as Durable Metal-free Catalysts for Iodine Reduction Reaction in Dye-sensitized Solar Cells. *Sci. Adv.* **2016**, 2, e1501459.
- (8) Liu, X.; Antonietti, M. Moderating Black Powder Chemistry for the Synthesis of Doped and Highly Porous Graphene Nanoplatelets and Their Use in Electrocatalysis. *Adv. Mater.* **2013**, 25, 6284-6290.

- (9) Jeon, I.-Y.; Zhang, S.; Zhang, L.; Choi, H.-J.; Seo, J.-M.; Xia, Z.; Dai, L.; Baek, J.-B. Edge-Selectively Sulfurized Graphene Nanoplatelets as Efficient Metal-Free Electrocatalysts for Oxygen Reduction Reaction: The Electron Spin Effect. *Adv. Mater.* **2013**, 25, 6138-6145.
- (10) Shao, Y.; Zhang, S.; Wang, C.; Nie, Z.; Liu, J.; Wang, Y.; Lin, Y. Highly Durable Graphene Nanoplatelets Supported Pt Nanocatalysts for Oxygen Reduction. *J. Power Sources* **2010**, 195, 4600-4605.
- (11) Russo, S.; Craciun, M. F.; Yamamoto, M.; Morpurgo, A. F.; Tarucha, S. Contact Resistance in Graphene-based Devices. *Phys. E* **2010**, 42, 677-679.
- (12) Min Song, S.; Yong Kim, T.; Jae Sul, O.; Cheol Shin, W.; Jin Cho, B. Improvement of Graphene-metal Contact Resistance by Introducing Edge Contacts at Graphene Under Metal. *Appl. Phys. Lett.* **2014**, 104, 183506.
- (13) Li, X.; Batchelor-McAuley, C.; Laborda, E.; Compton, R. G. Aqueous Voltammetry in the Near Absence of Electrolyte. *Chem. Eur. J.* **2017**, 23, 15222-15226.
- (14) Albery, W. J. *Electrode Kinetics*. Clarendon Press, 1975.
- (15) Cole, D. J.; Ang, P. K.; Loh, K. P. Ion Adsorption at the Graphene/Electrolyte Interface. *J. Phys. Chem. Lett.* **2011**, 2, 1799-1803.
- (16) Sarpoushi, M. R.; Borhani, M. R.; Nasibi, M.; Eghdami, B.; Kazerooni, H. Graphene Nanosheets as Electrode Materials for Supercapacitors in Alkaline and Salt Electrolytes. *Mater. Sci. Semicond. Process.* **2015**, 31, 195-199.
- (17) Davies, T. J.; Brookes, B. A.; Fisher, A. C.; Yunus, K.; Wilkins, S. J.; Greene, P. R.; Wadhawan, J. D.; Compton, R. G. A Computational and Experimental Study of the Cyclic Voltammetry Response of Partially Blocked Electrodes. Part II: Randomly Distributed and Overlapping Blocking Systems. *J. Phys. Chem. B* **2003**, 107, 6431-6444.
- (18) Sims, M. J.; Rees, N. V.; Dickinson, E. J. F.; Compton, R. G. Effects of Thin-layer Diffusion in the Electrochemical Detection of Nicotine on Basal Plane Pyrolytic Graphite (BPPG) Electrodes Modified With Layers of Multi-walled Carbon Nanotubes (MWCNT-BPPG). *Sens. Actuators, B* **2010**, 144, 153-158.
- (19) Lan, C.; Srisungsitthisunti, P.; Amama, P. B.; Fisher, T. S.; Xu, X. F.; Reifenger, R. G. Measurement of Metal/Carbon Nanotube Contact Resistance by Adjusting Contact Length Using Laser Ablation. *Nanotechnology* **2008**, 19, 125703.
- (20) Franklin, A. D.; Farmer, D. B.; Haensch, W. Defining and Overcoming the Contact Resistance Challenge in Scaled Carbon Nanotube Transistors. *ACS Nano* **2014**, 8, 7333-7339.
- (21) Krittayavathananon, A.; Li, X.; Batchelor-McAuley, C.; Sawangphruk, M.; Compton, R. G. Comparing the Effect of Different Surfactants on the Aggregation and Electrical Contact Properties of Graphene Nanoplatelets. *Applied Materials Today* **2018**, 12, 163-167.
- (22) Krittayavathananon, A.; Li, X.; Sokolov, S. V.; Batchelor-McAuley, C.; Sawangphruk, M.; Compton, R. G. The Solution Phase Aggregation of Graphene Nanoplates. *Applied Materials Today* **2018**, 10, 122-126.
- (23) Krittayavathananon, A.; Ngamchuea, K.; Li, X.; Batchelor-McAuley, C.; Kästelhön, E.; Chaisiwamongkhol, K.; Sawangphruk, M.; Compton, R. G. Improving Single-Carbon-Nanotube-Electrode Contacts Using Molecular Electronics. *J. Phys. Chem. Lett.* **2017**, 8, 3908-3911.
- (24) Li, X.; Batchelor-McAuley, C.; Shao, L.; Sokolov, S. V.; Young, N. P.; Compton, R. G. Quantifying Single-Carbon Nanotube-Electrode Contact via the Nanoimpact Method. *J. Phys. Chem. Lett.* **2017**, 8, 507-511.

- (25) Poon, J.; Batchelor-McAuley, C.; Tschulik, K.; Compton, R. G. Single Graphene Nanoplatelets: Capacitance, Potential of Zero Charge and Diffusion Coefficient. *Chem. Sci.* **2015**, 6, 2869-2876.
- (26) Gerischer, H.; McIntyre, R.; Scherson, D.; Storck, W. Density of the Electronic States of Graphite: Derivation from Differential Capacitance Measurements. *J. Phys. Chem.* **1987**, 91, 1930-1935.
- (27) Sun, S.; Qi, Y.; Zhang, T.-Y. Dissecting Graphene Capacitance in Electrochemical Cell. *Electrochim. Acta* **2015**, 163, 296-302.
- (28) Gouy, M. Sur la constitution de la charge électrique à la surface d'un électrolyte. *J. Phys. Theor. Appl.* **1910**, 9, 457-468.
- (29) Chapman, D. L. LI. A Contribution to the Theory of Electrocapillarity. *The London, Edinburgh, and Dublin Philosophical Magazine and Journal of Science* **1913**, 25, 475-481.
- (30) Vallés, C.; Drummond, C.; Saadaoui, H.; Furtado, C. A.; He, M.; Roubeau, O.; Ortolani, L.; Monthieux, M.; Pénicaud, A. Solutions of Negatively Charged Graphene Sheets and Ribbons. *J. Am. Chem. Soc.* **2008**, 130, 15802-15804.
- (31) Franks, G. V. Zeta Potentials and Yield Stresses of Silica Suspensions in Concentrated Monovalent Electrolytes: Isoelectric Point Shift and Additional Attraction. *J. Colloid Interface Sci.* **2002**, 249, 44-51.
- (32) Sokolov, S. V.; Eloul, S.; Kätelhön, E.; Batchelor-McAuley, C.; Compton, R. G. Electrode-particle Impacts: A Users Guide. *Phys. Chem. Chem. Phys.* **2017**, 19, 28-43.